

# Application of particle image velocimetry (PIV) to measure the displacement of sandy soil in laboratory

Tan-Phong Ngo<sup>1,2\*</sup>, Thuy-Chung Kieu-Le<sup>1,2</sup>

<sup>1</sup>Faculty of Geology and Petroleum Engineering, Ho Chi Minh city University of Technology

<sup>2</sup>Vietnam National University, Ho Chi Minh city

Received 1 March 2021; accepted 14 June 2021

## Abstract:

Particle image velocimetry (PIV) has been heavily used to measure the displacement and flow velocity in fluid mechanics. However, applications of this method to determining soil displacement in geotechnical laboratory tests are rare. This paper aims to verify the applicability of this method in determining the displacement of sandy soil under different saturation conditions and soil grain sizes. The results showed that this method could effectively determine soil displacement with an accuracy of 0.13 mm. Furthermore, the degree of saturation of soil did not influence the PIV results whereas the homogeneity of soil, as indicated by grain size distribution, reduced the precision of the PIV method.

**Keywords:** particle image velocimetry, sandy soil, soil displacement.

**Classification number:** 4.2

## Introduction

In geotechnical engineering, it is important to measure soil displacement in soil specimens for all laboratory tests, in physical models or in the field. This data is usually recorded using a strain gauge attached to the soil sample during the tests. With the availability of image analysis software, soil displacement analysis can be carried out easily and inexpensively using various image-based techniques such as X-ray, stereo-photogrammetric techniques, image processing, and PIV and each technique has its own advantages and limitations [1-4]. Among these techniques, PIV is an important non-invasive method to quantify local displacements on a solids' surface [5]. In this method, a series of successive images of an object are captured during the test without using any strain gauge sensors. By comparing the spatial variations on the same patches in these images using image analysis softwares, the displacement data can be obtained [6, 7]. PIV has been evidenced to be an effective technique for observation of stresses and strains of the glass ballotini and soil deformation in creep movement on the slope [4, 6, 8, 9]. In the present study, the PIV technique was adopted to predict the deformation of sandy soil with different degrees of saturation and soil grain size. The precision of the technique was verified

using displacement data recorded by a strain gauge during the tests.

## Materials and methods

### *Theory of the PIV method*

PIV is an important technique used in fluid dynamics (Fig. 1). It allows to obtain instantaneous velocity measurements and related properties at a specific area, called 'interrogation' areas, in the fluid [10]. PIV technique has its roots from the laser speckle velocimetry technique developed in the late 1970s [11, 12]. In PIV, the displacement of an interrogation area of a pair of digital images is calculated with help of cross-correlation or autocorrelation techniques. The cross-correlation functions are presented in Equations (1) to (3) below.

$$R(\underline{s}) = \sum_U I_{test}(\underline{U}) \cdot I_{search}(\underline{U} + \underline{s}) \quad (1)$$

$$N(\underline{s}) = \sum_U [I_{search}(\underline{U} + \underline{s}) \cdot I_{search}(\underline{U} + \underline{s})] \cdot M(\underline{U}) \quad (2)$$

$$R_n(\underline{s}) = \frac{R(\underline{s})}{N(\underline{s})} \quad (3)$$

where  $R(\underline{s})$  = cross-correlation matrix,  $N(\underline{s})$  = normalisation matrix,  $R_n(\underline{s})$  = normalized cross-correlation matrix,  $M(\underline{U})$  = dummy mask matrix,  $I_{test}(\underline{U})$  = intensity matrix of test patch,  $I_{search}(\underline{U} + \underline{s})$  = intensity matrix of search patch,  $\underline{U}$  and  $\underline{s}$  = pixel coordinate vector.

\*Corresponding author: Email: ngotanphong@hcmut.edu.vn

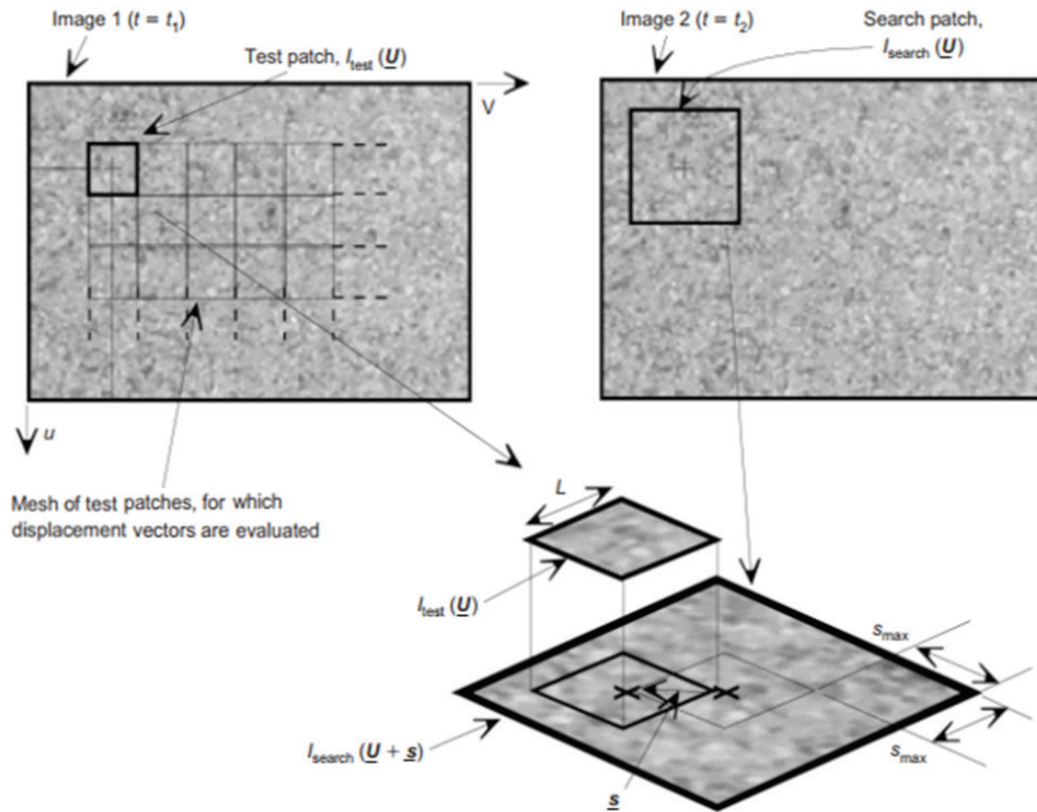


Fig. 1. Principles of image manipulation in PIV analysis [4].

**Testing materials**

The soil used in the test was yellow fine sand (Fig. 2A), which was air-dried until its water content of about 0.1%. According to the Unified soil classification system (USCS), the sand was classified as “SP” (i.e., poorly graded sand). The distribution of particle sizes was determined by the sieving method according to ASTM D422, and the grain size distribution curve is shown in

Fig. 2B.

Several physical and mechanical properties of the sand are presented in Table 1. The specific gravity was 2.65. The maximum dry density and optimum water content (ASTM D698) were  $16.7 \text{ kN/m}^3$  and 14.0%, respectively. The internal friction angle and cohesion (ASTM D3080) were  $38^\circ$  and 0 kPa, respectively. The average hydraulic conductivity of saturated sand at  $29^\circ\text{C}$ , i.e., ambient

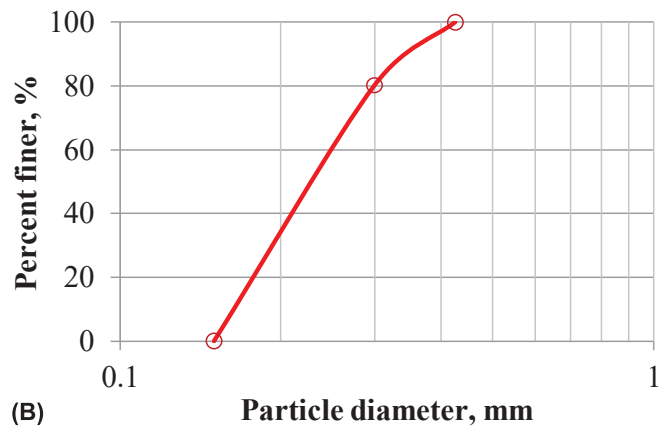
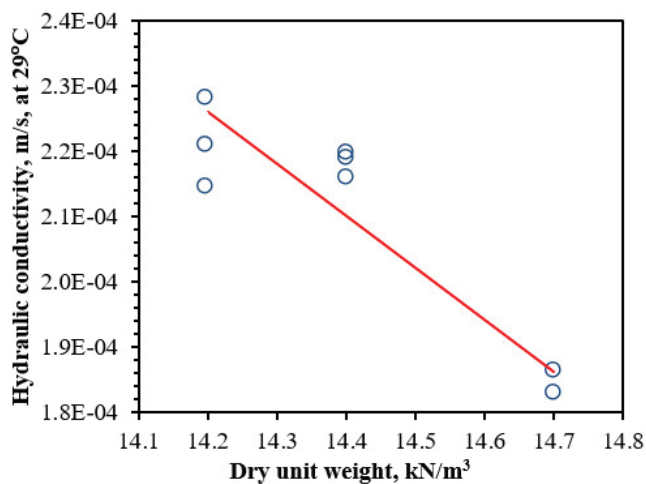


Fig. 2. Image of the poorly graded sand used in testing and its grain size distribution curve.

laboratory temperature, for dry unit weight varying from 14.2 to 16.7 kN/m<sup>3</sup>, which determined by the constant water head method ASTM D2434, was 2.1x10<sup>-4</sup> m/s and inversely proportional to the dry unit weight (Fig. 3).

**Table 1. Physical and mechanical properties of the sand.**

Properties	Value	Unit	Standard applied
Grain size distribution: sand - silt - clay	100-0-0	%	ASTM D422
D <sub>10</sub> , D <sub>30</sub> , D <sub>60</sub>	0.16-0.19-0.25	mm	-
Coefficient of uniformity, C <sub>u</sub>	1.5	-	-
Coefficient of curvature, C <sub>c</sub>	0.9	-	-
Classification	SP	-	ASTM D2487
Dry unit weight, γ <sub>d</sub>	14.5	kN/m <sup>3</sup>	ASTM D7263
Maximum dry unit weight, γ <sub>dmax</sub>	16.7	kN/m <sup>3</sup>	ASTM D698
Optimum water content, W <sub>opt</sub>	14.0	%	ASTM D698
Specific gravity, G <sub>s</sub>	2.65	-	ASTM D854
Cohesion, c'	0	kPa	ASTM D3080
Angle of internal friction, φ	38	°	ASTM D3080
Hydraulic conductivity, k <sub>sat</sub>	2.1x10 <sup>-4</sup>	m/s	ASTM D2434



**Fig. 3. Hydraulic conductivity variation with dry unit weight of saturated sand.**

**Experimental soil box**

An experimental soil box made of acrylic was designed and developed. This acrylic box consists of two parts: the upper box and the lower box. The upper box could slide easily while the lower box was attached firmly to the base. A bolt and a down gauge were used to move the upper box in the horizontal direction and the horizontal displacement could be measured (Fig. 4). There was also a guide located on the surface of the lower box to ensure the upper box could be moved easily. In order to calculate the ‘scale factor’ for PIV analysis, a steel ruler was attached to the lower box surface. The calibration process was also carried out on the same sand at different degrees of saturation from 0 to 90%. The camera Canon EOS REBEL T4i/EOS 650 was used for capturing the photos. The testing process was conducted carefully in a 3-m long, 2-m wide, and 2-m high ‘cell’ under the light conditions induced by two LED spotlights.

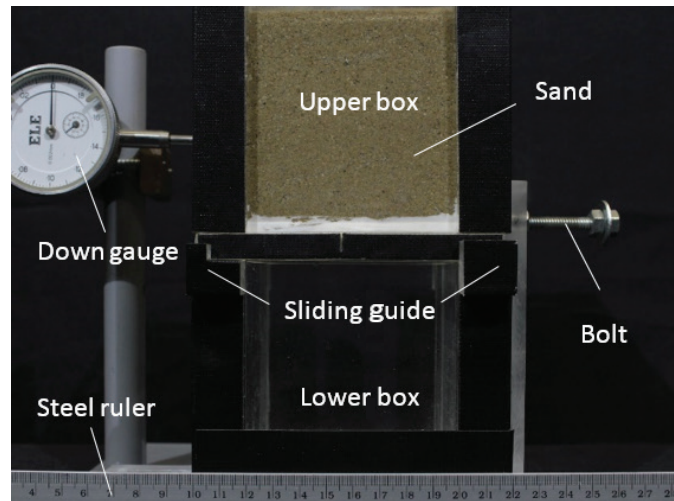


**Fig. 4. The acrylic testing soil box.**

**Experimental set-up**

The initial soil sample mentioned above, soil group A, had a particle size distribution that varied in the range of 0.85-0.15 mm. In order to evaluate the effect of particle distribution on PIV imaging results, group A was divided into 3 groups: group B (size range: 0.85-0.425 mm), group C (size range: 0.425-0.3 mm), and group D (size range: 0.3-0.15 mm). In addition, the effect of moisture on the results of the PIV image analysis were also evaluated for all four soil groups by moistening the soils to achieve the desired degrees of saturation.

A series of tests were carried out for each soil group by using the following experimental set-up:

1. Mix the soil with water to achieve the designed degree of saturation (S<sub>r</sub>=0, 20, 40, 60, 80, and 90%).

2. Put wet soil samples into the test box, compact the soil until the designed dry weight was attained (14.5 kN/m<sup>3</sup>).

3. And then move the upper part of the soil box at different intervals: 0.1, 0.2, 0.3, 0.4, 0.5, 0.6, 0.7, 0.8, 0.9, 1, 2, 3, 4, 5, 6, 7, and 8 mm and capture photos at every moving step.

Note that the distance from the camera to the test box was fixed at 40 and 80 cm to obtain the images of each condition with 2 different resolutions, 0.05 and 0.12 mm/pixel, respectively. In total, there were 48 experiments conducted for the four groups of soil particles in 6 different degrees of saturation with 2 image resolutions (Table 2).

The images captured after the experiments were analysed using OpenPIV image analysis software, developed by Taylor, et al. (2010) [2] in MATLAB, to obtain the displacement of the soil. OpenPIV is defaulted to use a given linear scaling factor, which is an input parameter, to convert the output data in pixel to real

sizes (prototype). In other words, the effect of distortion is neglected. Moreover, according to White (2002) [13], the distortion effect causes a small error compared to the random PIV error so it could be neglected when analysing the displacement measurement. The size of the interrogation area selected was 128 pixels × 128 pixels.

It should be noted that the output data from the OpenPIV are horizontal and vertical velocities. Therefore, the soil's displacement from movement was cumulatively calculated from both velocities multiplied by the displacement time.

**Results and discussion**

*Horizontal displacement*

A series of successive images captured during the experiments were analysed using the OpenPIV image analysis software to obtain the soil's horizontal displacement at intervals of 0.1, 1, 2, 3, 4, and 5 mm as presented in Fig. 5. As described previously, only

**Table 2. Soil particle size, degree of saturation, and image scaling factor for the 48 experimental set-ups.**

Soil type	Scaling factor (mm/pixel)	Degree of saturation, S <sub>r</sub> %					
		0	~20	~40	~60	~80	~90
A (0.85-0.15 mm)	0.05	✓	✓	✓	✓	✓	✓
	0.12	✓	✓	✓	✓	✓	✓
B (0.85-0.425 mm)	0.05	✓	✓	✓	✓	✓	✓
	0.12	✓	✓	✓	✓	✓	✓
C (0.425-0.3 mm)	0.05	✓	✓	✓	✓	✓	✓
	0.12	✓	✓	✓	✓	✓	✓
D (0.3-0.15 mm)	0.05	✓	✓	✓	✓	✓	✓
	0.12	✓	✓	✓	✓	✓	✓

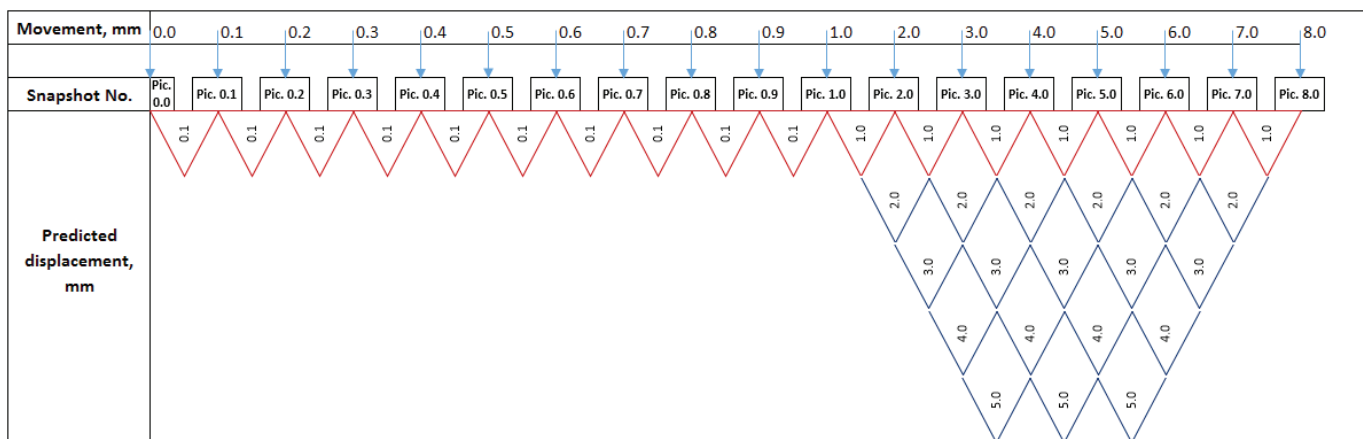


**Fig. 5. Scheme of interpreting the horizontal displacement using PIV method.**

horizontal deformation in the soil sample was allowed. Therefore, the total displacement is equal to the horizontal displacement. Fig. 6 shows an image of the movement vector of the soil after moving the upper box at a distance of 1 mm in the horizontal direction.

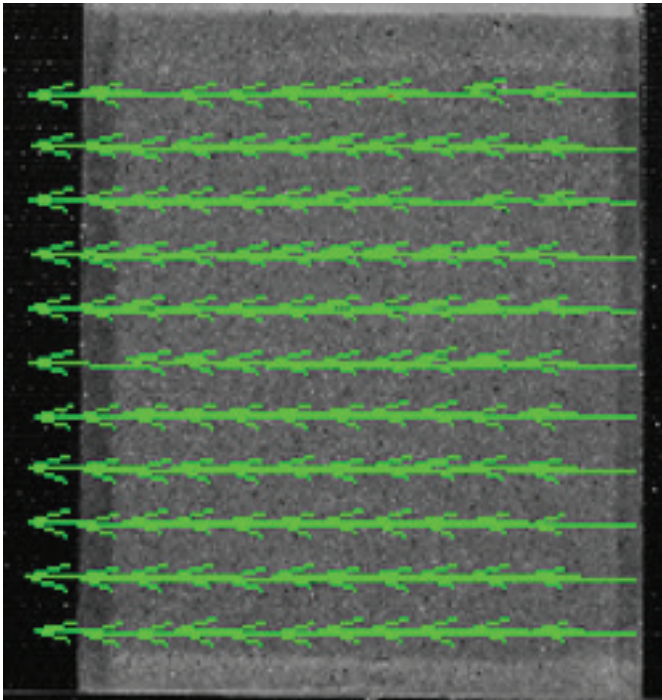


Fig. 6. Horizontal displacement of sand.

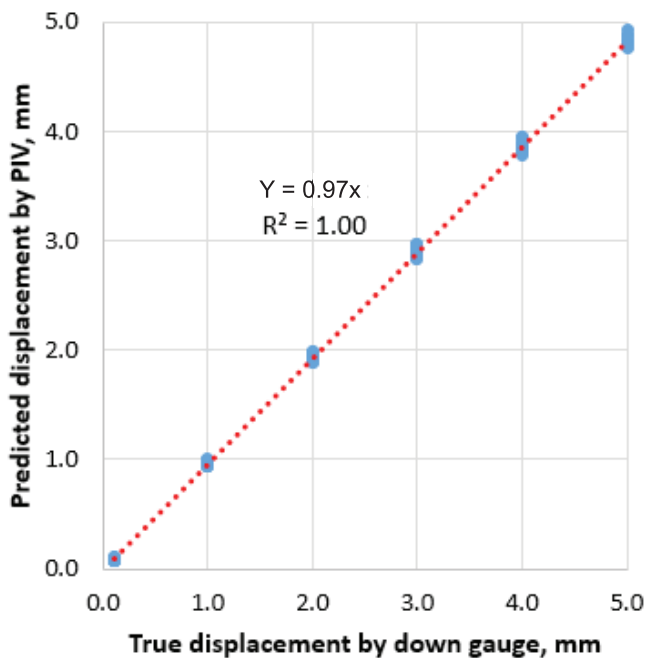


Fig. 7. Correlation between predicted displacement and true displacement.

Figure 7 presents the relationship between the predicted displacement determined from PIV and true displacement measured by the down gauge. Their correlation function was given by Equation (4) with the coefficient of determination  $R^2=1.0$ , which indicates that the predicted displacement from PIV was equivalent to the true displacement.

$$\text{Predicted displacement} = 0.97 \times \text{True displacement} \quad (4)$$

### Accuracy

The predicted horizontal displacements of the soil sample were also determined by OpenPIV software for interval values ranging from 0.1 to 5 mm corresponding to the four soil groups A, B, C, and D. The accuracy of the predicted displacement was calculated using the following equation:

$$\text{Accuracy} = | \text{True displacement} - \text{Predicted displacement} | \quad (5)$$

For the four soil groups A, B, C, and D, there were no considerable differences in the accuracy of predicted displacement (Fig. 8). The accuracy varied from 0.02 mm (soil A,  $S_r=74\%$ ) to 0.24 mm (soil B in dry condition, i.e.  $S_r=0$ ) with an average accuracy of 0.13 mm.

Considering the accuracy in the same soil group as the degree of saturation was increased, the variation of the accuracy did not show any clear pattern or trend. Therefore, the effect of saturation could be ignored when analysing PIV results.

In all four soil groups A, B, C, and D, with the same test patch size of 128 pixels  $\times$  128 pixels used in the interpretation process, the image with the scaling factor of 0.12 mm/pixel gave a smaller accuracy value than the image with scaling factor of 0.05 mm/pixel. This can be explained by the fact that the area of the test patch of the 0.12 mm/pixel image is larger than the 0.05 mm/pixel image, so the results of PIV interpretation are more accurate.

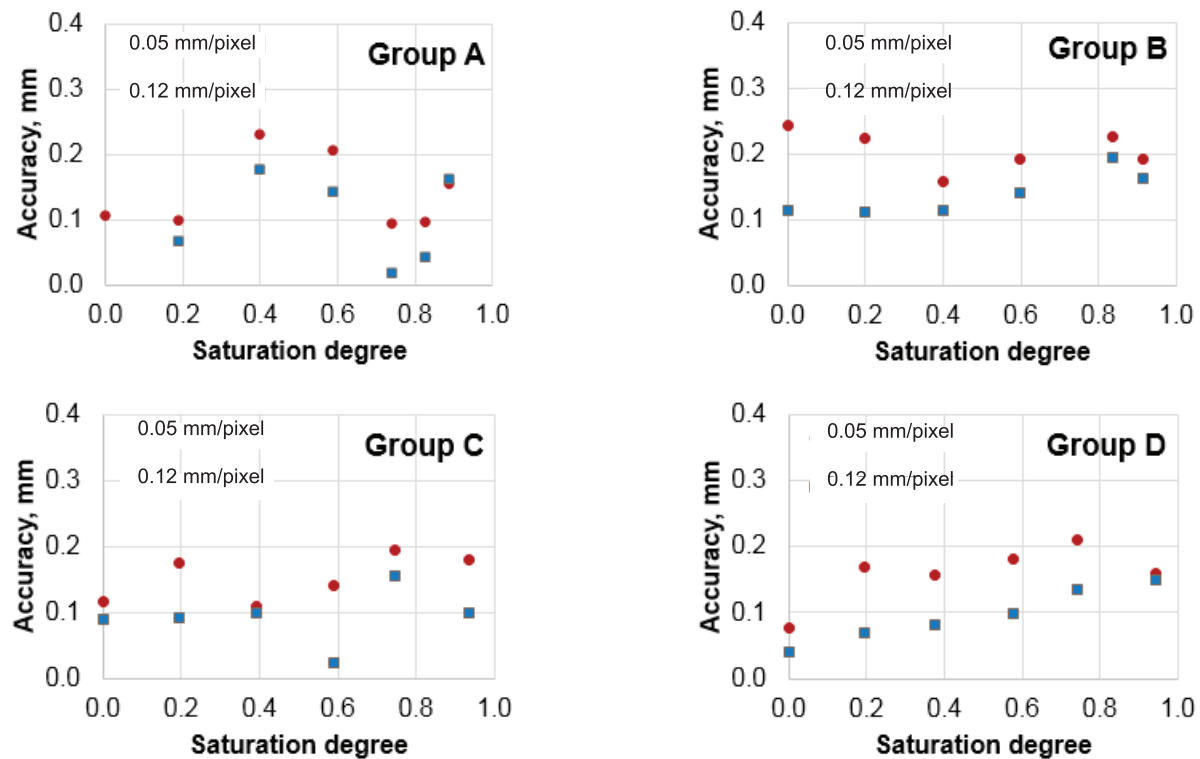


Fig. 8. Change of accuracy with saturation degree for the four sample groups.

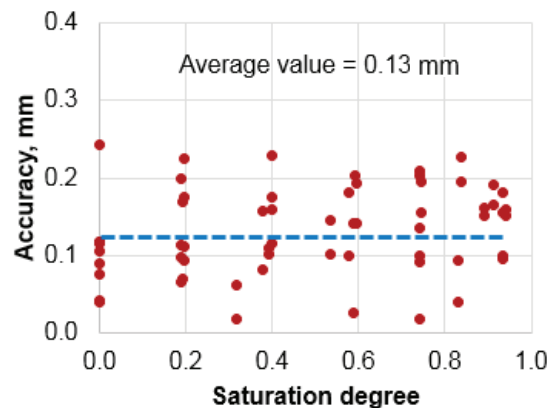


Fig. 9. Average accuracy in the measurement range of 0.1 to 5 mm.

The average accuracies of PIV for the measurement intervals from 0.1 to 5 mm were also determined as the average value of all separate accuracy values. As shown in Fig. 9, the average accuracy was 0.13 mm.

### Precision

The precision of the predicted displacement obtained

from PIV was defined as the standard error of the predicted displacement. The precision values for all experimental setups for the four soil groups are shown in Fig. 10. Soil group A, which contained the larger particle grain sizes, presented quite low precision when compared to the other soil groups indicating that the more homogeneous the soil, the more scattered the predicted displacement.

Considering the effect of the degree of saturation of soil for all soil groups, there did not appear to be much difference in the precision as the degree of saturation of soil changed. Therefore, the variation of soil's degree of saturation did not affect the scattering of the results predicted from PIV.

In all four soil groups A, B, C, and D, with the same test patch size of 128 pixels  $\times$  128 pixels used in the interpretation process, the image with scaling factors of 0.05 and 0.12 mm/pixel gave precision values of 0.002 and 0.01 mm, respectively.

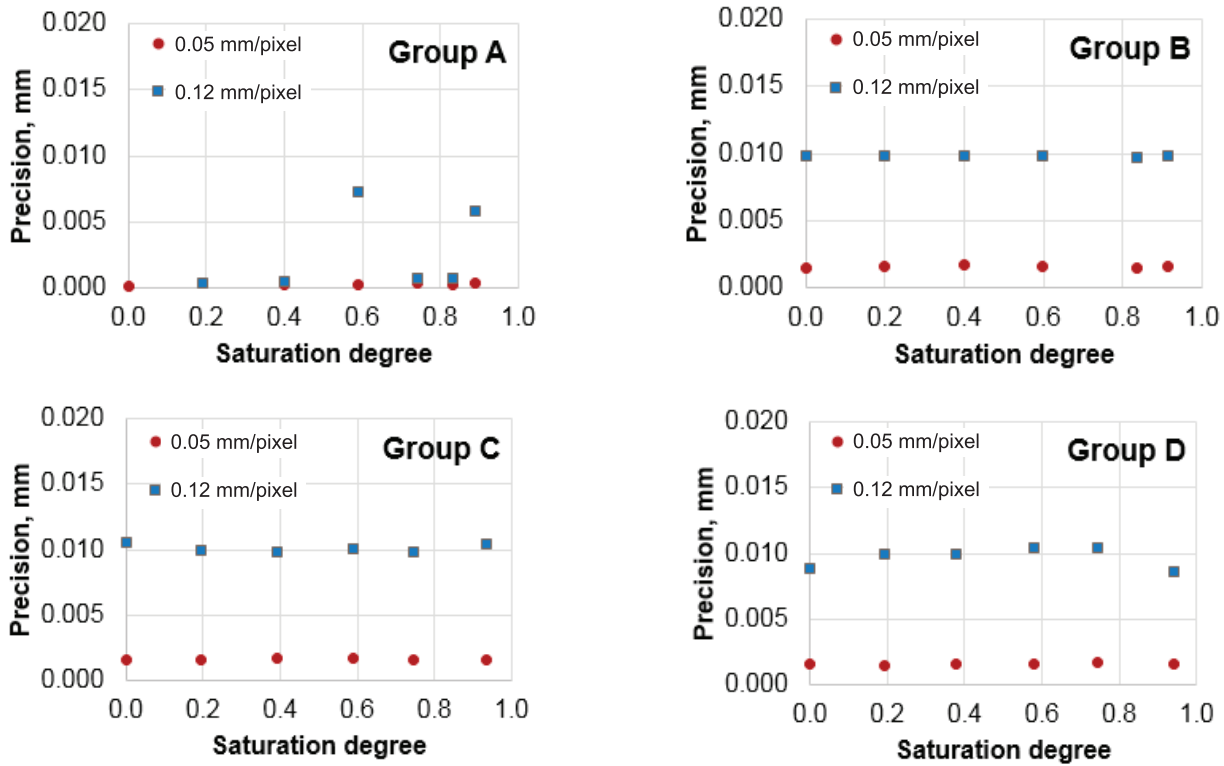


Fig. 10. Change of precision with saturation degree for the four sample groups.

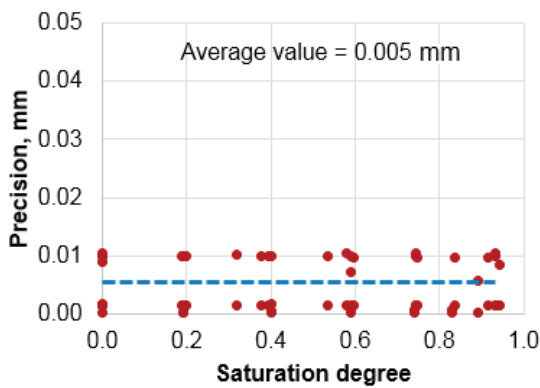


Fig. 11. Average precision in the measurement range of 0.1 to 5 mm.

The average precision values of PIV for measurement intervals from 0.1 to 5 mm were also determined as the average value of all separate precision values. As shown in Fig. 11, the average precision was 0.005 mm.

**Conclusions**

The results showed that in the measurement ranges of 0.1 to 5 mm with image scaling factors of 0.05 and

0.12 mm/pixel, the average values of accuracy and precision were 0.13 and 0.005 mm, respectively. This study also evidenced that PIV can be used to predict the displacement of sandy soil. The results also showed that while the degree of saturation of the soil did not influence the PIV results, and can therefore be ignored when analysing PIV results, the homogeneity of soil could reduce the precision of the PIV method. In other words, PIV works effectively for more heterogeneous soil when grain size distribution is concerned.

**ACKNOWLEDGEMENTS**

This research is funded by Ho Chi Minh city University of Technology (HCMUT) under grant number T-DCDK-2019-32.

**COMPETING INTERESTS**

The authors declare that there is no conflict of interest regarding the publication of this article.

## REFERENCES

- [1] K.H. Roscoe, J.R.F. Arthur, R.G. James (1963), "Determination of strains in soils by X-ray method", *Civil Engineering and Public Works Review*, **58**, pp.873-876.
- [2] R.N. Taylor, R. Gurka, G.A. Kopp, A. Liberzon (2010), "Long-duration time-resolved piv to study unsteady aerodynamics", *Instrumentation and Measurement*, **59(12)**, pp.3262-3269, DOI: 10.1109/TIM.2010.2047149.
- [3] S. Paikowsky, F. Xi (2000), "Particle motion tracking utilizing a high-resolution digital CCD camera", *Geotechnical Testing Journal*, **23(1)**, pp.123-134, DOI: 10.1520/GTJ11130J.
- [4] D.J. White, W.A. Take, M.D. Bolton (2003), "Soil deformation measurement using particle image velocimetry (PIV) and photogrammetry", *Geotechnique*, **53(7)**, pp.619-632.
- [5] C. Slominski, M. Niedostatkiewicz, J. Tejchman (2007), "Application of particle image velocimetry (PIV) for deformation measurement during granular silo flow", *Powder Technology*, **173(2007)**, pp.1-18.
- [6] D. Lesniewska, D.M. Wood (2009), "Observations of stresses and strains in a granular material", *Journal of Engineering Mechanics*, **135(9)**, pp.1038-1054, DOI: 10.1061/ASCEEM.1943-7889.0000015.
- [7] M.R. Abdi, H. Mirzaefair (2017), "Experimental and PIV evaluation of grain size and distribution on soil-geoid interactions in pullout test", *Soils and Foundation*, **57**, pp.1045-1058.
- [8] H.O. Baba, S. Peth (2021), "Large scale soil box test to investigate soil deformation and creep movement on slopes by particle image velocimetry (PIV)", *Soil & Tillage Research*, **125(2012)**, pp.38-43, DOI: 10.1016/j.still.2012.05.021.
- [9] T.P. Ngo, S. Likitlersuang, A. Takahashi (2019), "Performance of a geosynthetic cementitious composite mat for stabilising sandy slopes", *Geosynthetics International*, **1-33**, DOI: 10.1680/jgein.19.00020.
- [10] R.J. Adrian (1991), "Particle-imaging techniques for experimental fluid mechanics", *Annual Review of Fluid Mechanics*, **23(1991)**, pp.261-304, DOI: 10.1146/annurev.fl.23.010191.001401.
- [11] J.C. Dainty (1975), *Laser Speckle and Related Phenomena*, 280pp, Springer-Verlag Berlin Heidelberg, Germany.
- [12] R. Butterfield, R.M. Harkness, K.Z. Andrews (1970), "A stereo-photogrammetric method for measuring displacement fields", *Geotechnique*, **20(3)**, pp.308-314, DOI: 10.1680/geot.1970.20.3.308.
- [13] D.J. White (2002), *An Investigation into the Behaviour of Pressed in Piles*, Ph.D. dissertation, University of Cambridge.